# X-rays from Magnetic Massive Stars

David Cohen
Swarthmore College

motivated by the MiMeS Delawareland meeting and preparation of the ipod paper

# X-ray Properties: are magnetic stars distinguished from non-magnetic stars?

1. X-ray luminosity: over-luminous?
2. Harder X-rays: hotter plasma from MCWS?
3. Emission lines: narrower due to confinement?
4. Variability: rotational modulation plus stochastic?

*are magnetic O stars distinct from magnetic B stars?*

# 1. X-ray Luminosity

## All magnetic O stars are overluminous

(compared to the $L_x \sim 10^{-7} L_{bol}$ relationship seen in normal O stars)

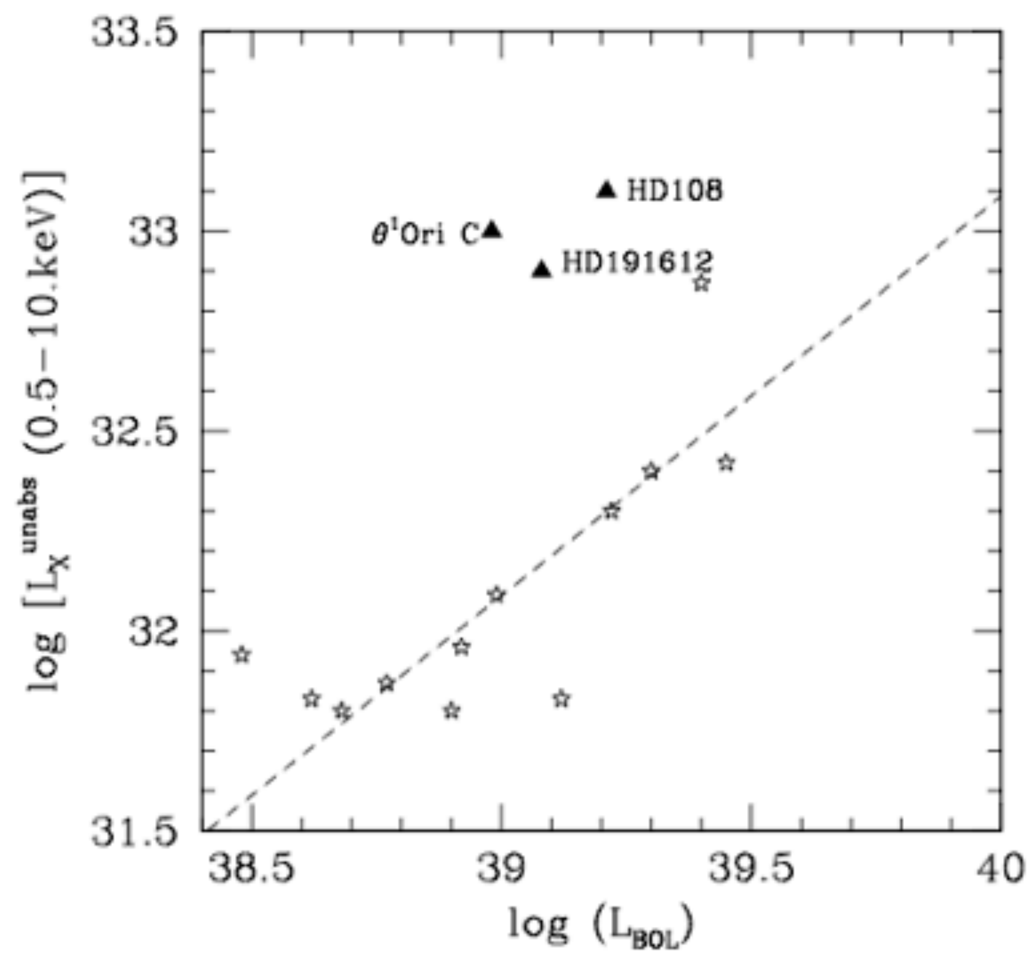


**Figure 4.** Diagram showing the X-ray luminosity (in erg $s^{-1}$) versus bolometric luminosity (in erg $s^{-1}$). The dashed line indicates the typical relation for O stars (from Sana et al. 2006); HD 108, HD 191612 and $\theta^1$ Ori C all lie above it. Asterisks show the position of hot stars in NGC 6231 (Sana et al. 2006) with three outliers: the two objects lying above the line are CW binaries whereas the one lying below is a Wolf–Rayet binary.

Can we put the other ~5 magnetic O stars on this plot?

Nazé et al., 2007, MNRAS, 375, 145

# 1. X-ray Luminosity

## Some B stars are overluminous (but the behavior of “normal” B stars’ $L_x/L_{bol}$ is complex; steeply declining from $10^{-7}$ with decreasing $T_{eff}$)

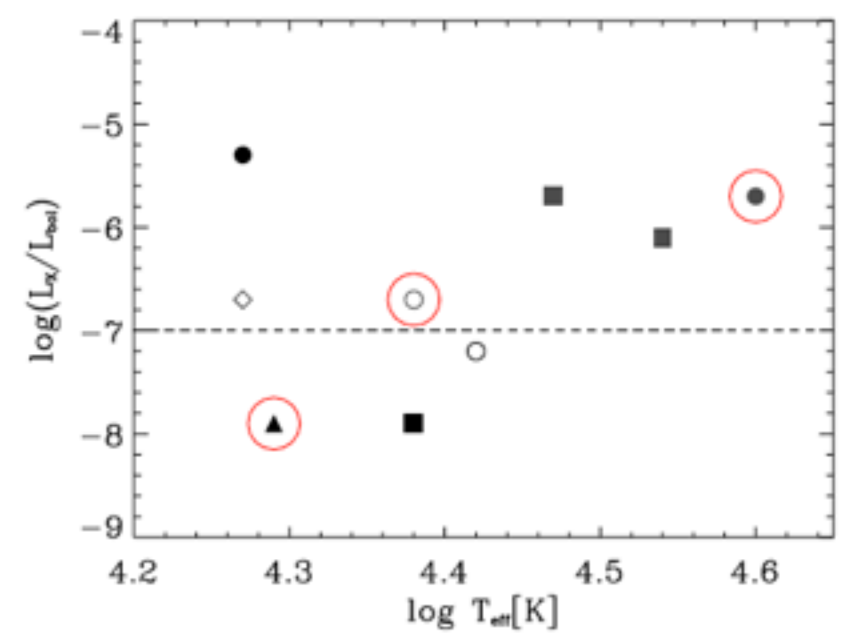


Figure 1. X-ray efficiency of the ONC massive stars as a function of effective temperature. The stars in which fields are detected are circled. *Filled symbols* are for stars with indirect indications of the presence of a magnetic field and *grey symbols* are for confirmed or suspected binaries. Plotting symbols indicate the following properties: *squares* are for stars showing possible X-ray rotational modulation, *circles* are for T Tauri type X-ray emission, *triangles* are chemically peculiar (CP) stars, and the *diamond* star was not observed. The *dotted line* indicates the typical efficiency for massive stars.

Petit et al., 2009, ASPC, 405, 547

# 1. X-ray Luminosity

## Some B stars are overluminous

(but the behavior of "normal" B stars' $L_x/L_{bol}$ is complex; steeply declining from $10^{-7}$ with decreasing $T_{eff}$)

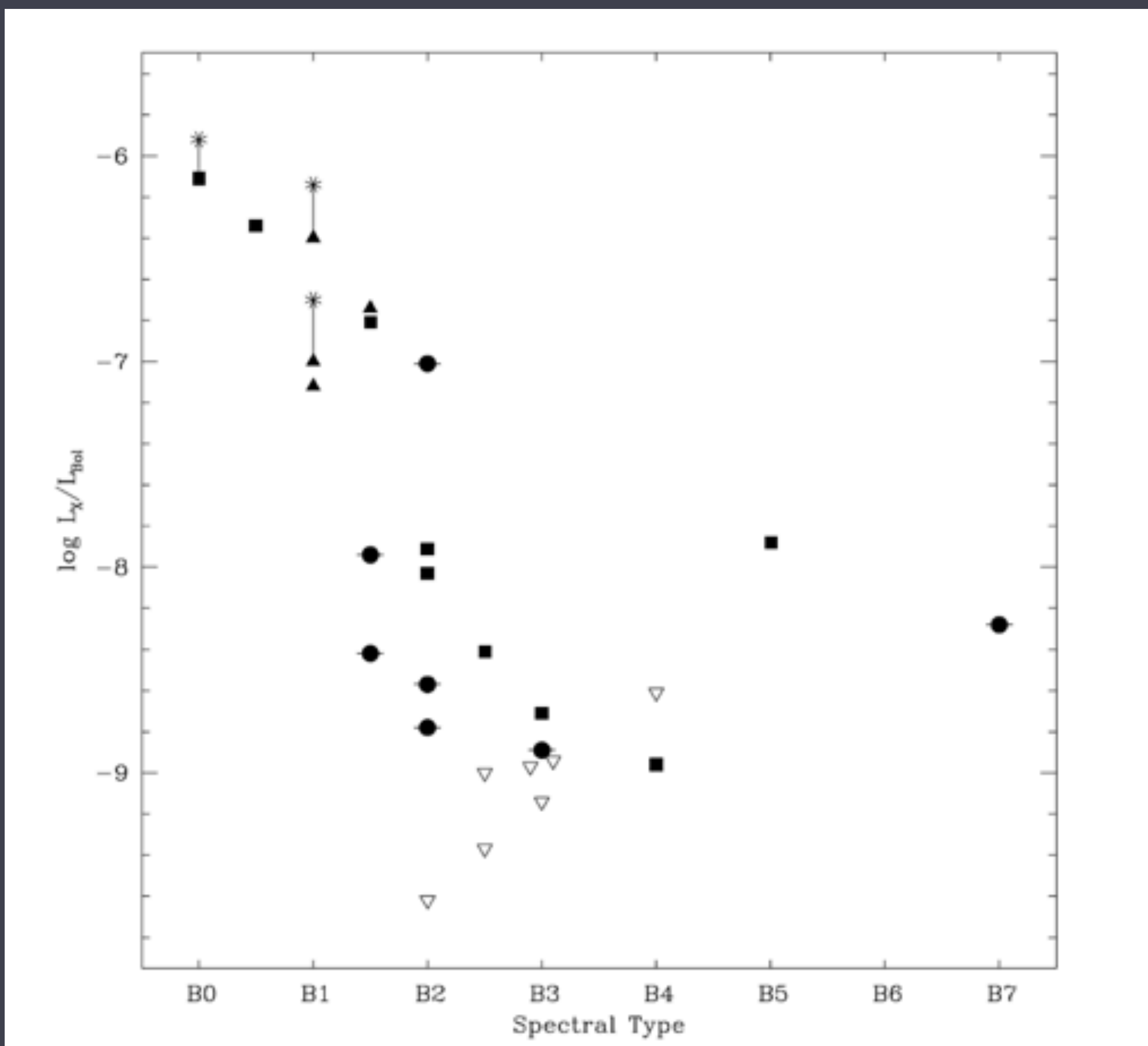


Cohen, Cassinelli, & MacFarlane, 1997, ApJ, 487, 867

What $L_x$ or $L_x/L_{bol}$ is required for a B star to be considered *overluminous* in X-rays?

FIG. 2.—The ratio $L_X/L_{Bol}$ for each of the 20 program stars that were detected above the 3 $\sigma$ level. For three stars, $\tau$ Sco, $\beta$ Cen, and $\xi^1$ CMa, we indicate the total generated luminosities with asterisks, which are connected to the points, representing the emergent X-ray luminosities, by a line. The upper limits (3 $\sigma$) for seven stars are indicated with open triangles. Be stars are indicated by filled circles with lines, and $\beta$ Cephei variables by filled triangles.

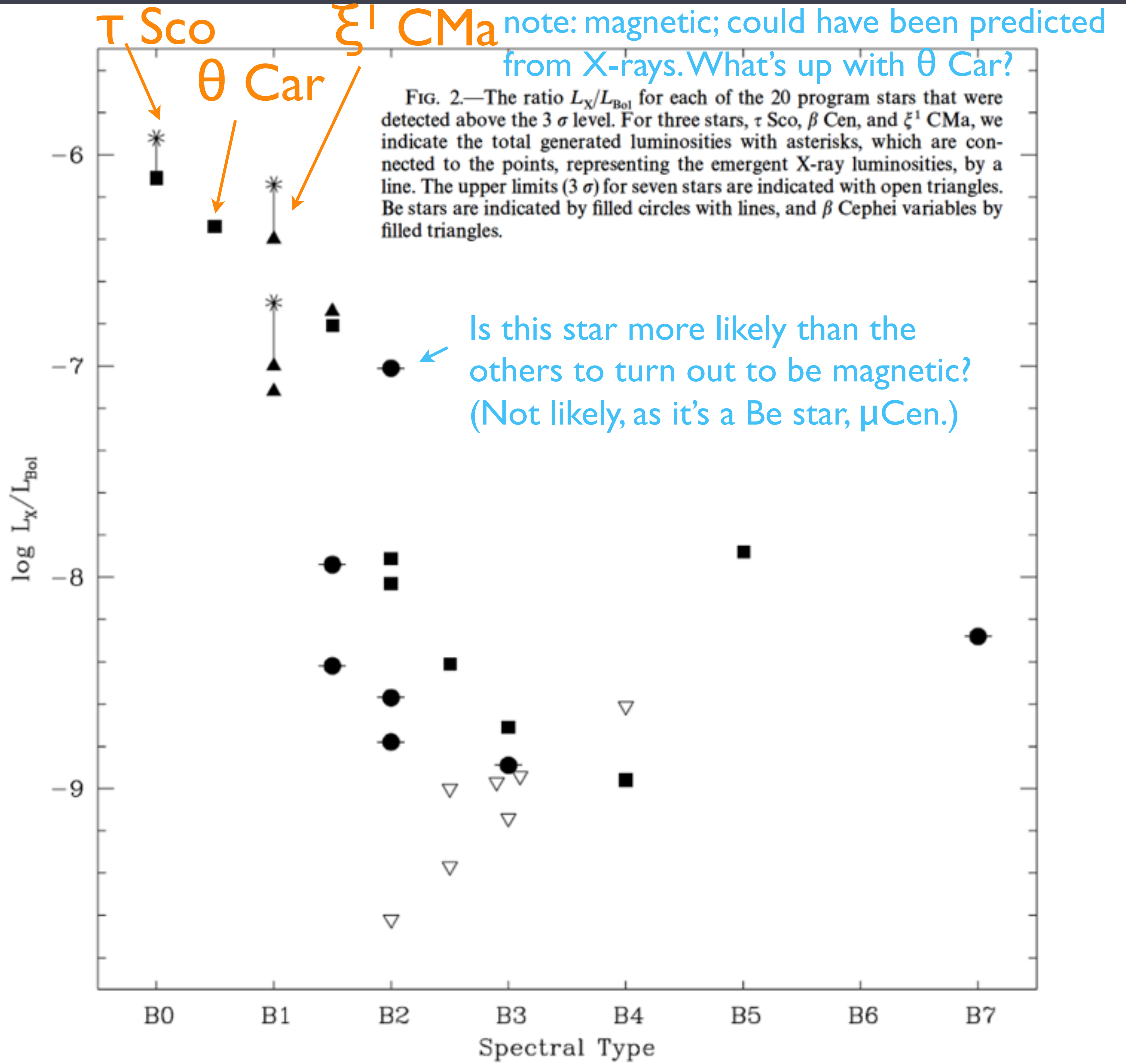


FIG. 2.—The ratio $L_X/L_{Bol}$ for each of the 20 program stars that were detected above the 3 $\sigma$ level. For three stars, $\tau$ Sco, $\beta$ Cen, and $\xi^1$ CMa, we indicate the total generated luminosities with asterisks, which are connected to the points, representing the emergent X-ray luminosities, by a line. The upper limits (3 $\sigma$) for seven stars are indicated with open triangles. Be stars are indicated by filled circles with lines, and $\beta$ Cephei variables by filled triangles.

Cohen, Cassinelli, & MacFarlane, 1997, ApJ, 487, 867

# 1. X-ray Luminosity

Some B stars are overluminous
(but the behavior of "normal" B stars' $L_x/L_{bol}$ is complex; steeply declining from $10^{-7}$ with decreasing $T_{eff}$)

**Table 1.** Magnetic early B-type stars with available X-ray observations

| Name | HD | Sp | $B^a$ G | $v \sin i$ km s$^{-1}$ | $P_{rot}$ d | Dipole | Obliquity$^b$ $\beta$ | Ref |
|---|---|---|---|---|---|---|---|---|
| $\tau$ Sco | 149438 | B0V | $\langle\sim 500\rangle$ | 5 | 41.033 | no | | *1* |
| | | | $\beta$ Cep-type and SPB-type stars | | | | | |
| $\xi^1$ CMa | 46328 | B0.7IV | $5300 \pm 1100$ | $9 \pm 2$ | 2.18 | yes | 79.1 | *2* |
| $\beta$ Cep | 205021 | B2III | $360 \pm 40$ | $27 \pm 2$ | 12.00089 | yes | $85° \pm 10°$ | *3, 4* |
| V2052 Oph | 163472 | B1V | $250 \pm 190$ | $60 \pm 4$ | 3.63883 | yes | $35° \pm 18°$ | *5* |
| $\zeta$ Cas | 3360 | B2IV | $335^{+120}_{-65}$ | $17 \pm 3$ | 5.37045 | yes | $77° \pm 6°$ | *6* |
| | | | Peculiar B stars | | | | | |
| NU Ori | 37061 | B0V(n) | $\sim$620 | $225 \pm 50$ | | yes | | *7* |
| V1046 Ori | 37017 | B2V | $\langle\sim 1500\rangle$ | $\lesssim$95 | 0.9 | ? | 42°–59° | *8, 9, 13* |
| HR 3089 | 64740 | B1.5Vp | $\langle 572 \pm 114\rangle$ | 160 | 1.33 | ? | | *9, 13, 14* |
| LP Ori | 36982 | B2Vp | $\sim$1100 | $80 \pm 20$ | | yes | | *7* |
| $\sigma$ Ori E | 37479 | B2Vp | $\sim$10000 | $140 \pm 10$ | 1.191 | yes | 66° | *10* |
| HR 5907 | 142184 | B2.5Ve | $\sim$20000 | 280 | 0.5083 | yes(?) | 4° (?) | *11, 12* |

[a] for dipole field configuration, B is the polar field strength.
For $\tau$ Sco, HR 3089, and V1046 Ori, an approximate average field strength is shown in angle brackets
[b] $\beta$ is the angle between the magnetic and rotational axes for the dipole field configuration
*References: 1* Donati et al. (2006); Sota et al. (2011); *2* Hubrig et al. (2011); *3* Telting et al. (1997); *4* Donati et al. (2001); *5* Neiner et al. (2003b) *6* Neiner et al. (2003a); *7* Petit et al. (2008); *8* Bohlender et al. (1987); *9* Romanyuk & Kudryavtsev (2008); *10* Reiners et al. (2000); *11* Abt et al. (2002); *12* Grunhut et al. (2010); *13* Bychkov et al. (2003); *14* Borra & Landstreet (1979)

Oskinova et al., 2011, MNRAS, 416, 1456

# 1. X-ray Luminosity

## Some B stars are overluminous (but the behavior of "normal" B stars' $L_x/L_{bol}$ is complex; steeply declining from $10^{-7}$ with decreasing $T_{eff}$)

**Table 4.** X-ray luminosities of magnetic early B-type stars

| Name | d pc | $L_X$ $10^{30}$ erg s$^{-1}$ | $\log(L_X/L_{bol})$ |
|---|---|---|---|
| $\tau$ Sco | 150 | 40 | -6.4 |
| Magnetic $\beta$ Cep-type and SPB-type stars | | | |
| $\xi^1$ CMa | 420 | 30 | -6.6 |
| $\beta$ Cep | 200 | 6.4 | -7.0 |
| V2052 Oph | 400 | 0.3 | -8.0 |
| $\zeta$ Cas | 180 | 0.5 | -7.5 |
| Other magnetic early-type B stars | | | |
| NU Ori | 400 | 1.0 | -8 |
| V1046 Ori[a] | 380 | 0.1 | -8.0 |
| $\sigma$ Ori E[b] | 640 | 80 | -5.6 |
| HR 3089[c] | 300 | 2 | -7.2 |
| LP Ori | 470 | 0.02 | -8.5 |
| HR 5907 | 120 | 0.4 | -7.4 |

Distances are from van Leeuwen (2007) except of LP Ori, $\sigma$ Ori E, HR 3089;
[a] the distance between the X-ray source;
2XMM J053522.0-042938 and the position of V1046 Ori is 3″;
[b] $L_X$ (quiescent+flare) in 0.1-2.4 keV band from Sanz-Forcada et al. (2004) ;
[c] $L_X$ in 0.1-2.4 keV band from Drake et al. (1994);

Oskinova et al., 2011, MNRAS, 416, 1456

see these values plotted on the next slide

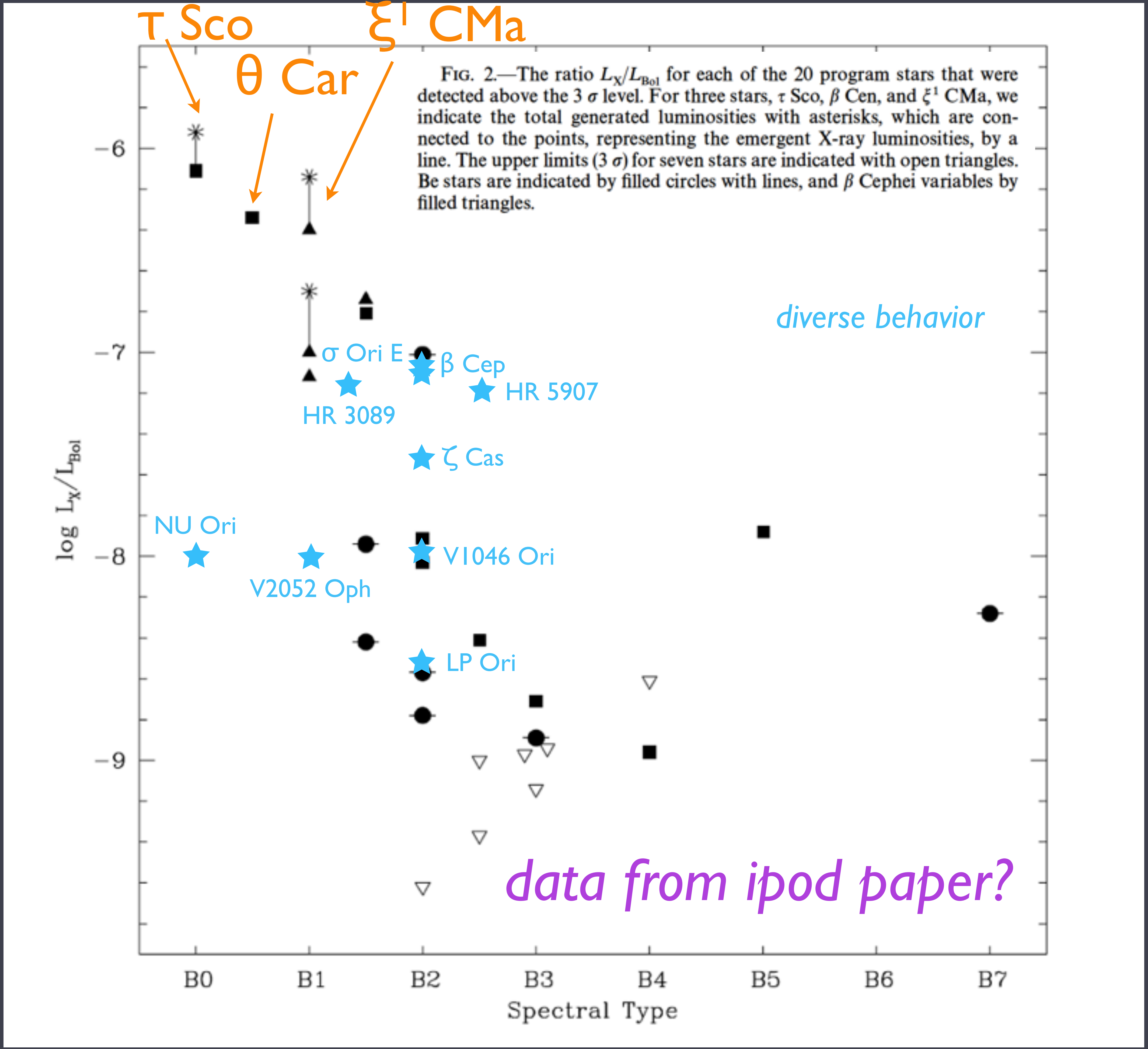


Cohen, Cassinelli, & MacFarlane, 1997, ApJ, 487, 867

# 1. X-ray Luminosity

What do we know about the $L_x$ and $L_x/L_{bol}$ values of the confirmed magnetic OB stars?

*Maybe only the O stars are consistently over-luminous in X-rays*

# II. X-ray Hardness & Plasma Temperature

## naive MCWS expectation is for stronger shocks, higher temperatures, and hard X-rays

## $\theta^1$ Ori C: prototype magnetic O star

hotter than seen in EWS

temperature

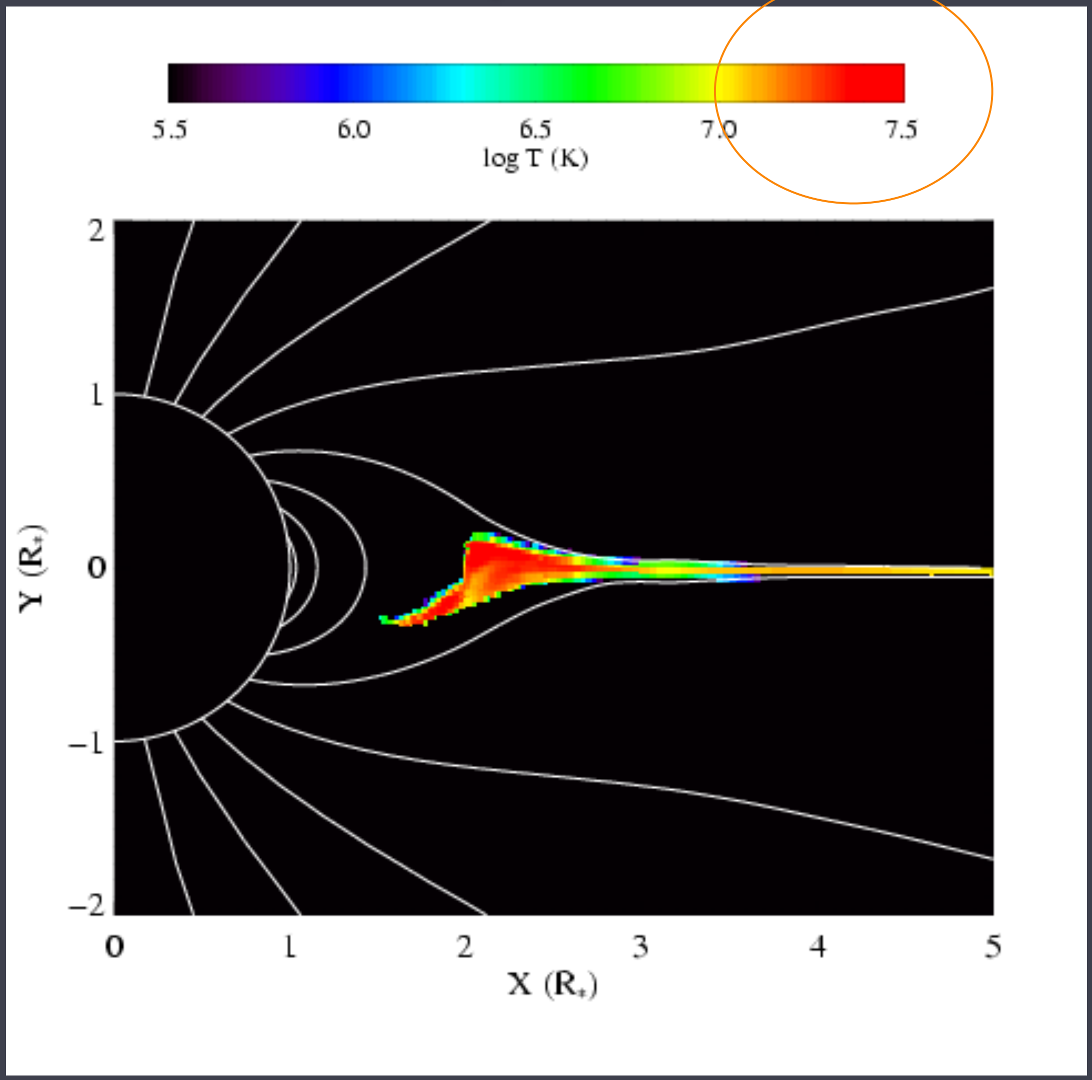


emission measure

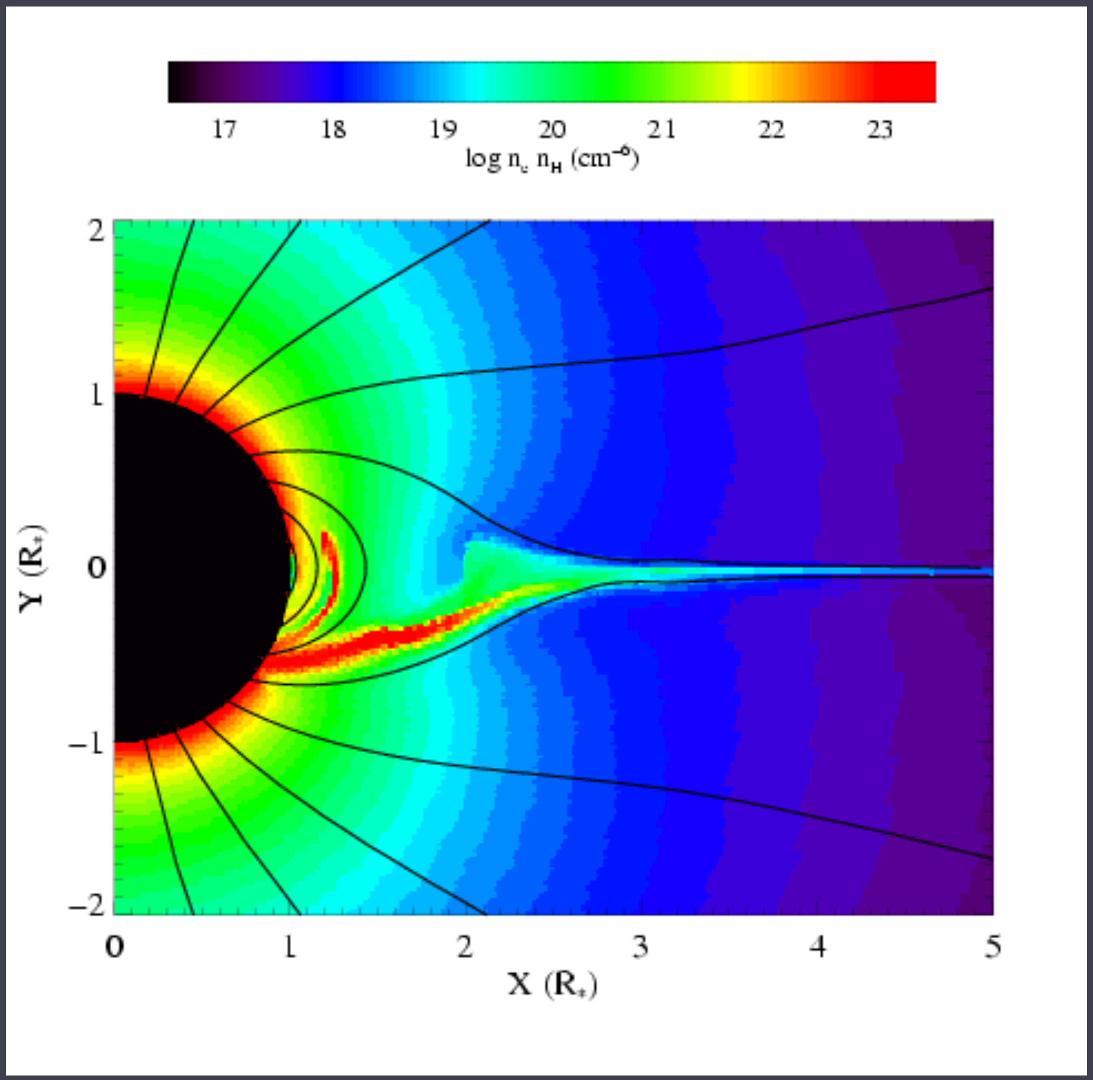


simulations by A. ud-Doula; Gagné et al. (2005)

# $\theta^1$ Ori C: hotter plasma than prototypical EWS source

## Mg XII / Mg XI is proportional to temperature

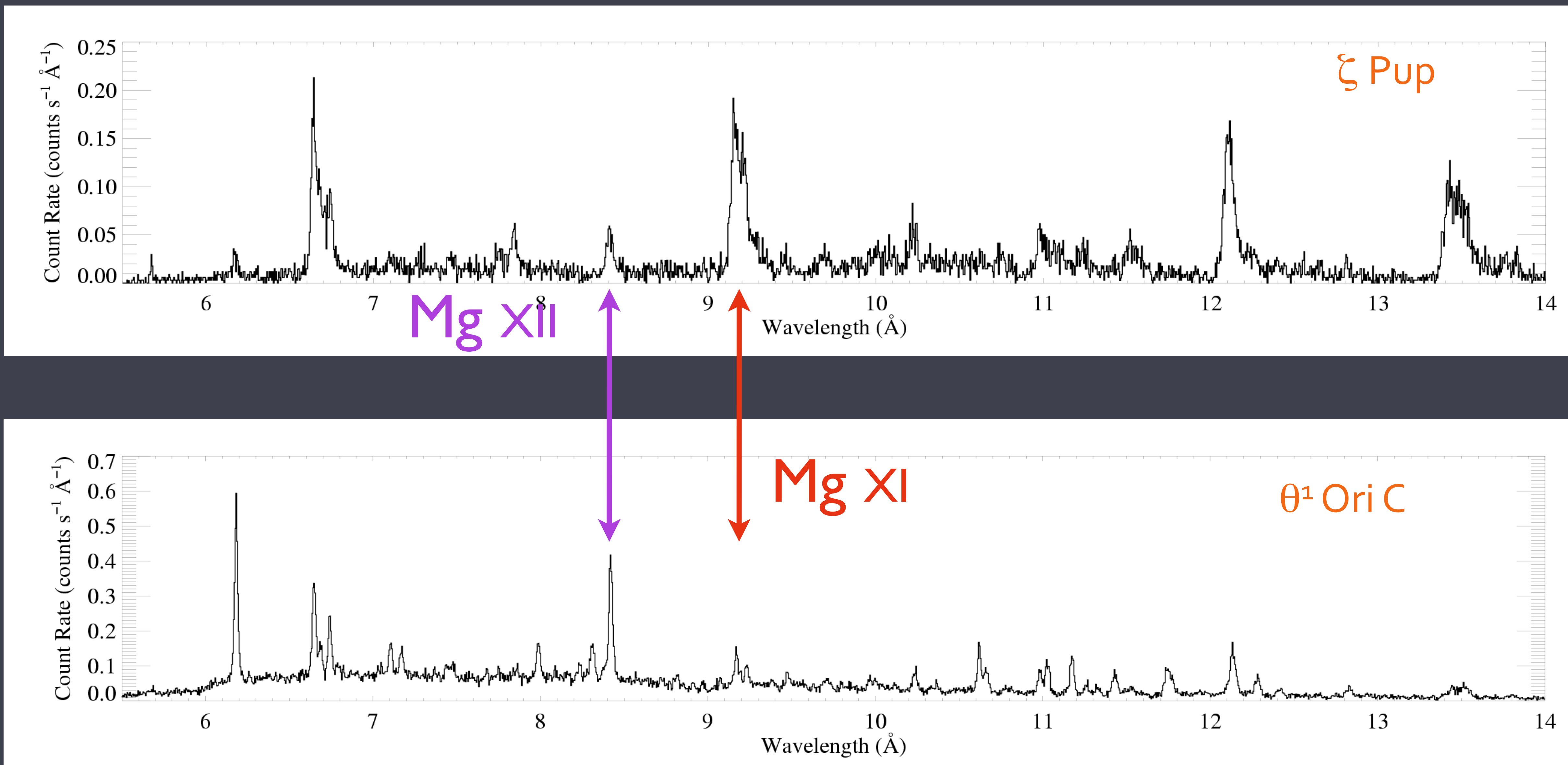

# other magnetic O stars (Of?p stars) have softer spectra, but still harder than EWS sources

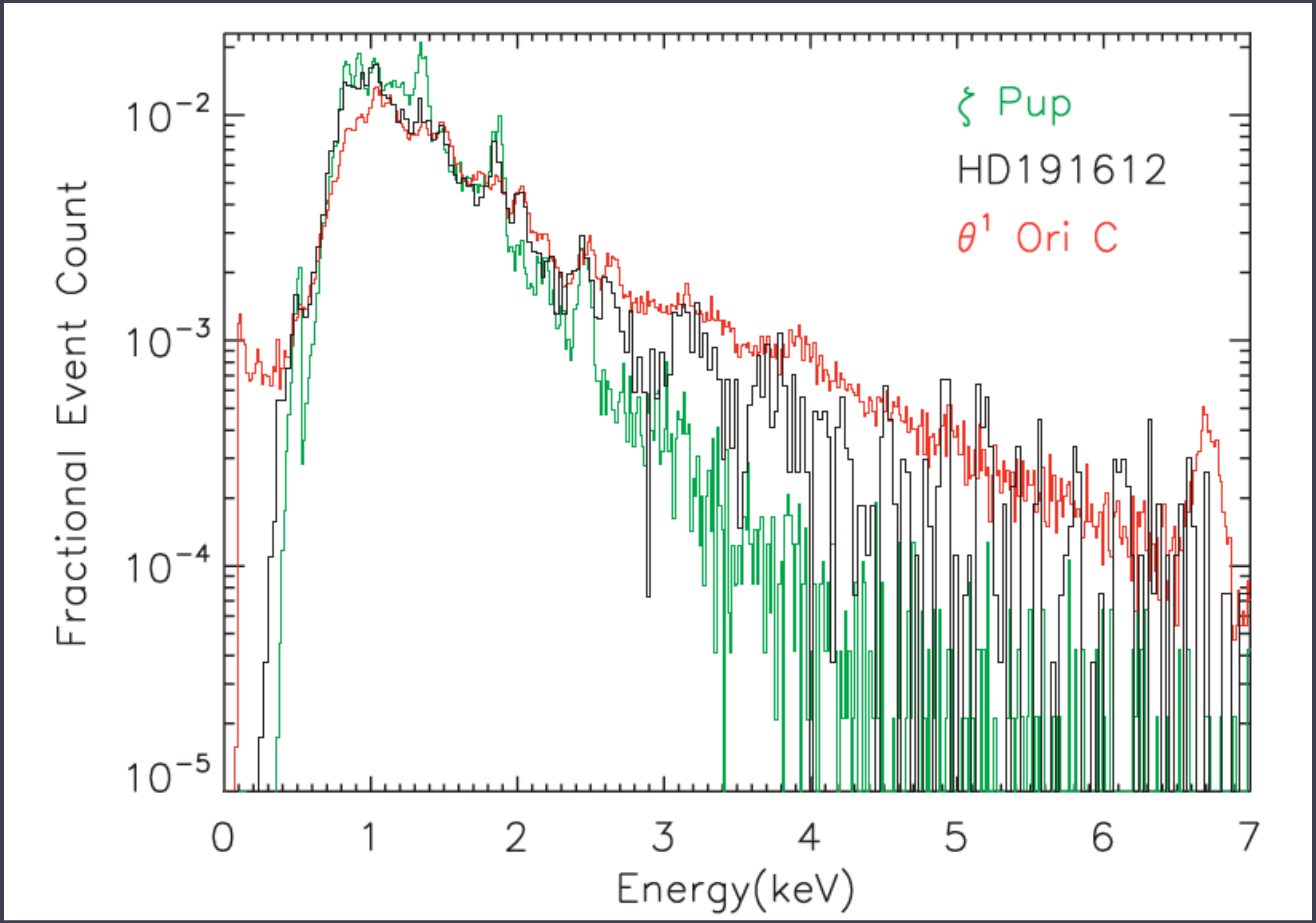


Nazé et al., 2007, MNRAS, 375, 145

# and a small but measurable amount of high-temperature plasma

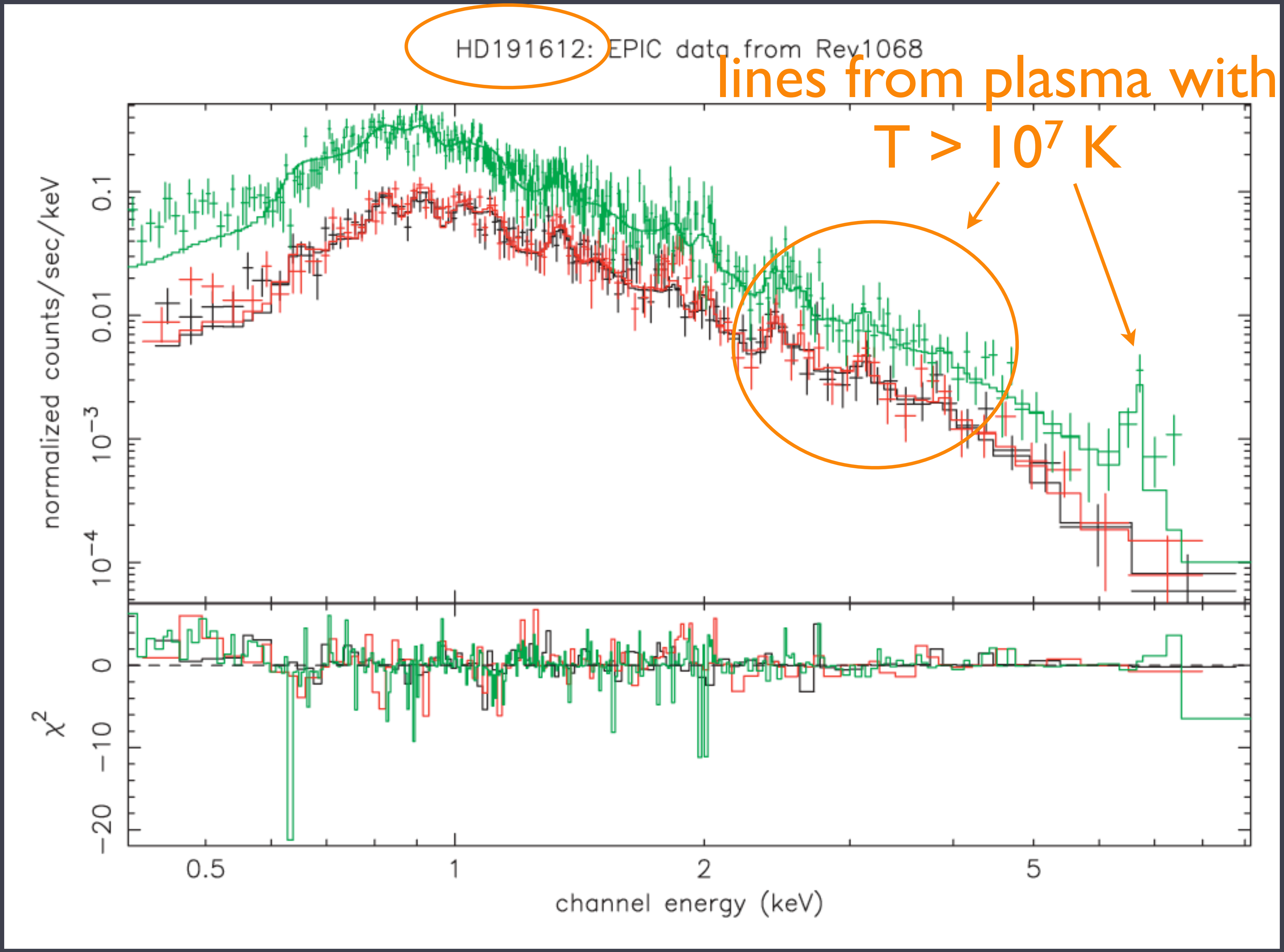


Nazé et al., 2007, MNRAS, 375, 145

# II. X-ray Hardness & Plasma Temperature

## Some hotter plasma in HD 191612, but it dominates in $\theta^1$ Ori C

### HD 191612: few million K

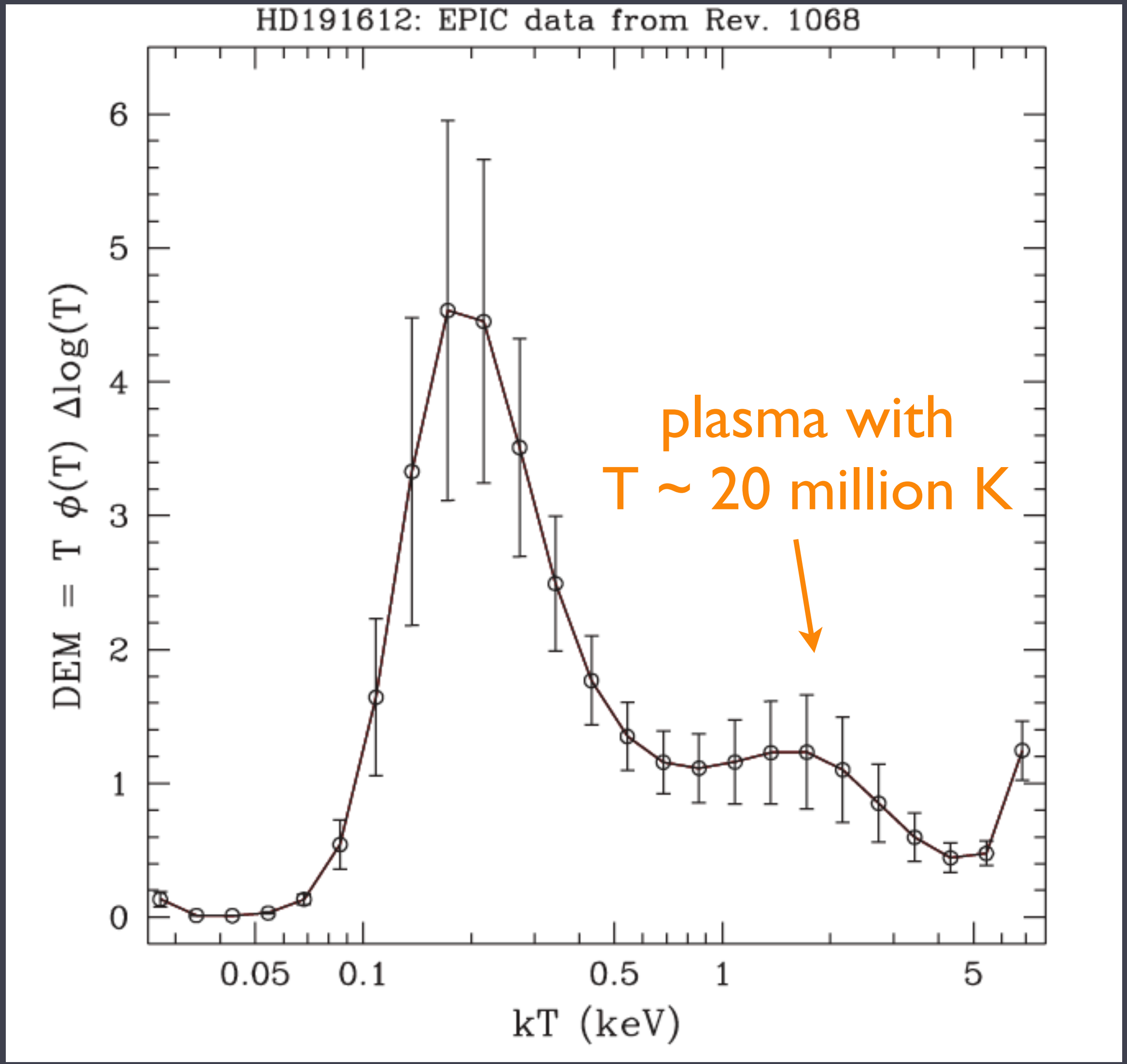


Nazé et al., 2007, MNRAS, 375, 145

### $\theta^1$ Ori C: 40 million K

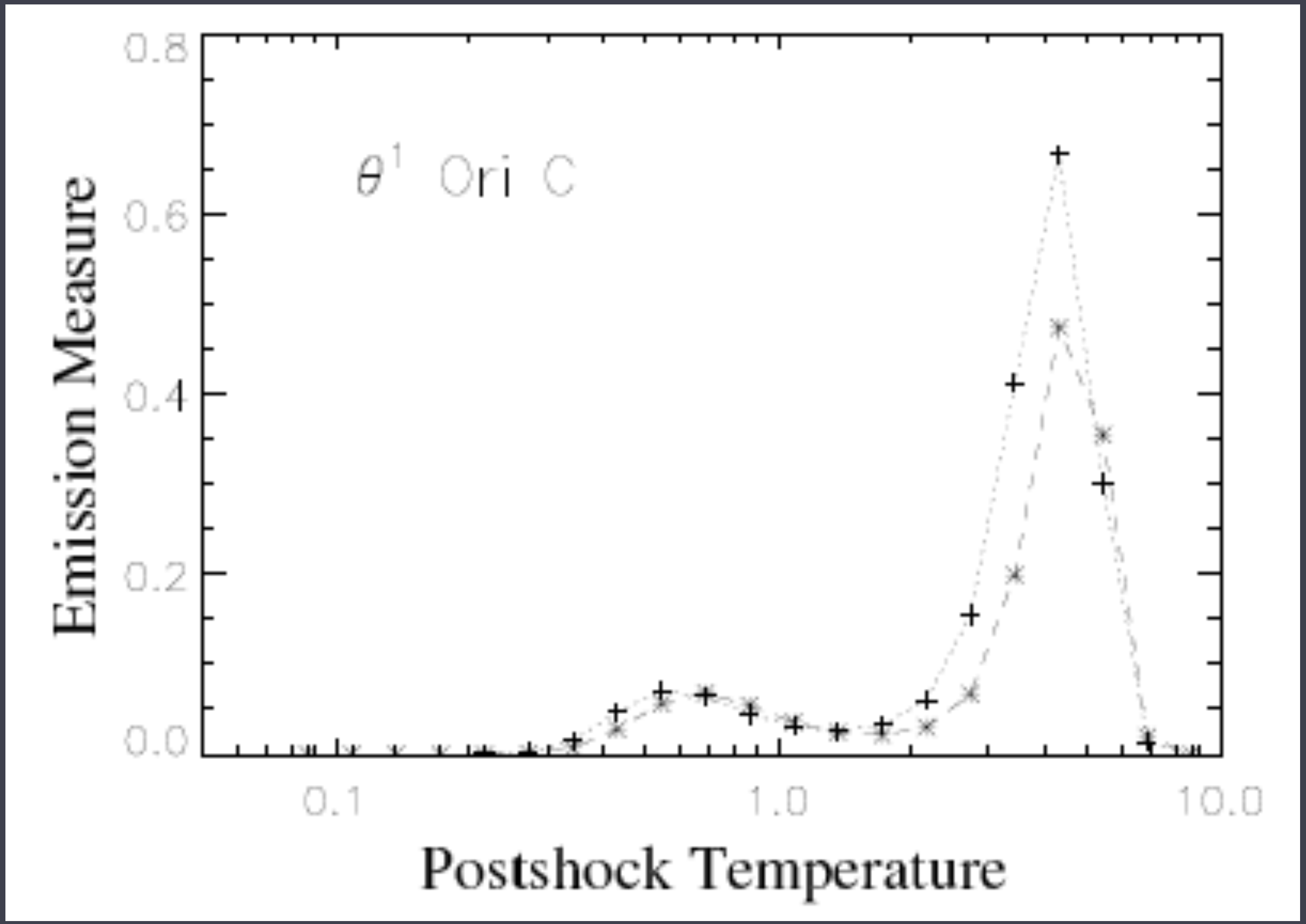


Zhekov & Palla, 2007, MNRAS, 375, 145

# plasma temperature distributions of selected OB stars

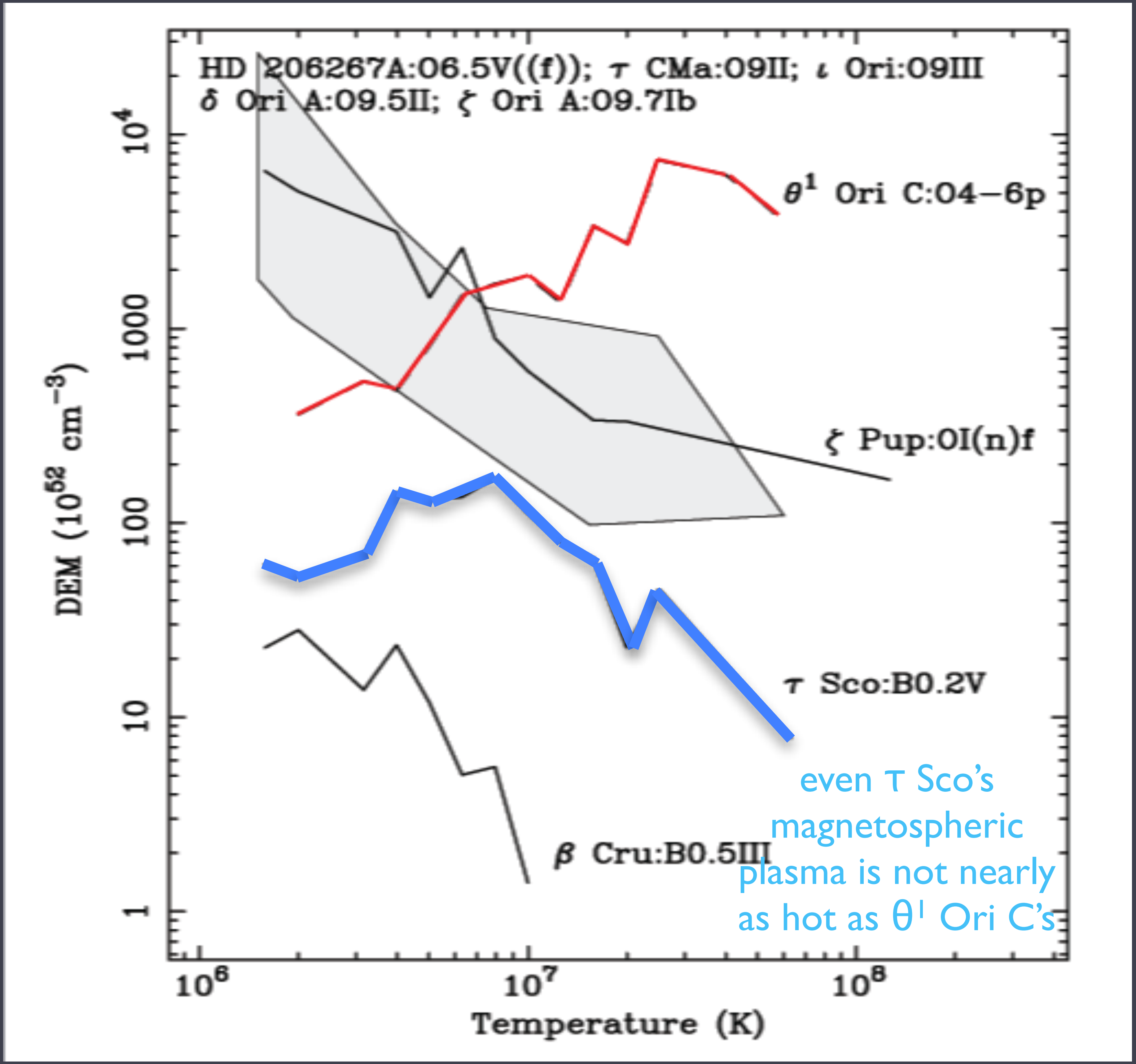


Wojdowski & Schulz, 2005, ApJ, 627, 953

# some magnetic B stars have low plasma temperatures

## though there *may* be some hotter plasma present

**Table 3.** The spectral parameters derived from the *XMM-Newton* EPIC observations of our program stars assuming the multi-temperature CIE plasma models (*vapec*) corrected for the interstellar absorption (*tbabs*). The values which have no error have been frozen during the fitting process. The corresponding spectral fits are shown in Figs. 1,3,2. For comparison, the spectral parameters inferred from modeling *XMM-Newton* data of $\beta$ Cep and *Suzaku* spectra of $\tau$ Sco are also shown.

| Star | $\xi^1$ CMa | $\zeta$ Cas | V2052 Oph | $\beta$ Cep[a] | $\tau$ Sco[b] |
|---|---|---|---|---|---|
| $N_{\rm H}^{\rm c}$ [$10^{20}$ cm$^{-2}$] | 1.4 | 3 | 15 | $2.5 \pm 0.1$ | 3 |
| $kT_1$ [keV] | $0.12 \pm 0.01$ | $0.08 \pm 0.02$ | $0.14 \pm 0.12$ | $0.24 \pm 0.01$ | $0.11 \pm 0.01$ |
| EM$_1$ [$10^{53}$cm$^{-6}$] | $22.48 \pm 5.64$ | $1.29 \pm 1.05$ | $0.006 \pm 0.025$ | $11 \pm 2$ | $17.0 \pm 2.61$ |
| $kT_2$ [keV] | $0.32 \pm 0.01$ | $0.31 \pm 0.02$ | | | $0.34 \pm 0.01$ |
| EM$_2$ [$10^{53}$cm$^{-3}$] | $19.3 \pm 3.36$ | $0.27 \pm 0.07$ | | | $10.4 \pm 0.51$ |
| $kT_3$ [keV] | $0.68 \pm 0.05$ | | $0.65 \pm 0.11$ | $0.69 \pm 0.03$ | $0.71 \pm 0.10$ |
| EM$_3$ [$10^{53}$ cm$^{-6}$] | $6.41 \pm 2.57$ | | $0.003 \pm 0.002$ | $1.3 \pm 0.3$ | $7.2 \pm 0.3$ |
| $kT_4$ [keV] | | | | | $1.52 \pm 0.06$ |
| EM$_4$ [$10^{53}$ cm$^{-6}$] | | | | | $5.2 \pm 0.3$ |
| $\langle kT \rangle \equiv \sum_i kT_i \cdot {\rm EM}_i / \sum_i {\rm EM}_i$ [keV] | 0.3 | 0.1 | 0.3 | 0.3 | 0.5 |
| Flux[d] [$10^{-12}$ erg cm$^{-2}$ s$^{-1}$] | 1.1 | 0.093 | 0.006 | 1.0 | 16.4 |

[a] the values are adopted from Favata et al. (2009)

[b] the values are adopted from Ignace et al. (2010)

[c] correspond to the ISM hydrogen column density for all stars

[d] in the 0.3-7.0 keV band, except of $\tau$ Sco in the 0.3-10.0 keV band, absorbed;

Oskinova et al., 2011, MNRAS, 416, 1456

# II. X-ray Hardness & Plasma Temperature

current status: *rather diverse behavior among magnetic massive stars; but some degree of enhanced hot plasma in many objects.*

hypothesis: weaker winds have weaker shocks, perhaps related to cooling lengths

# III. X-ray emission line widths and plasma kinematics

## $\theta^1$ Ori C shows narrow lines compared to $\zeta$ Pup

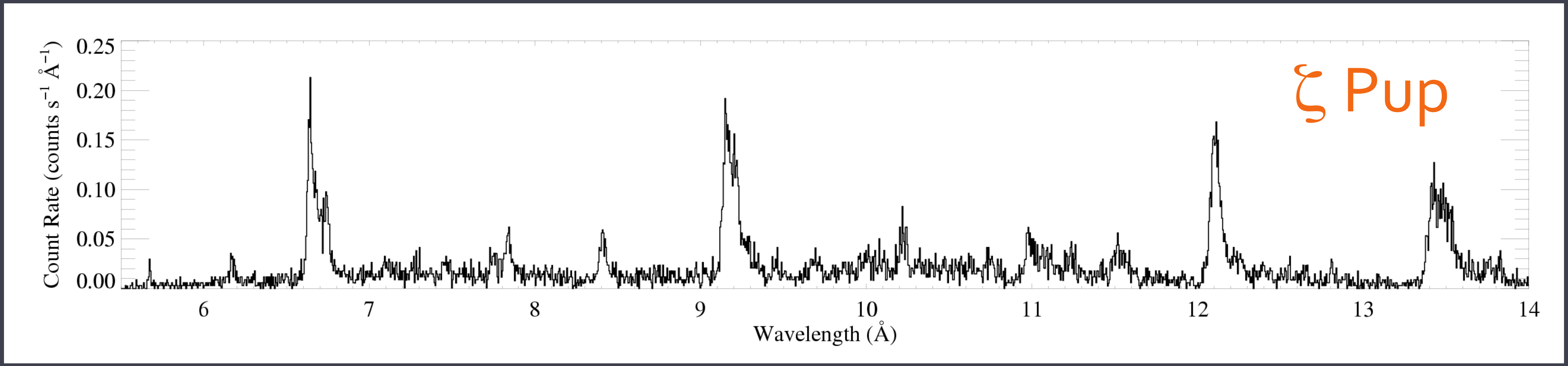


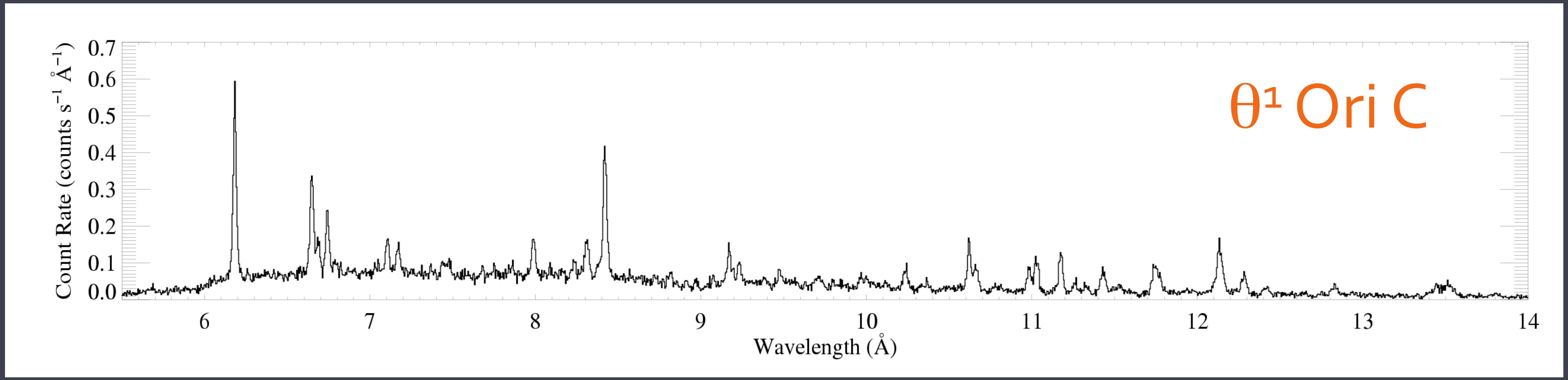

# III. X-ray emission line widths and plasma kinematics

## θ[1] Ori C shows narrow lines, at least for those lines formed in the hotter (> $10^7$K) plasma

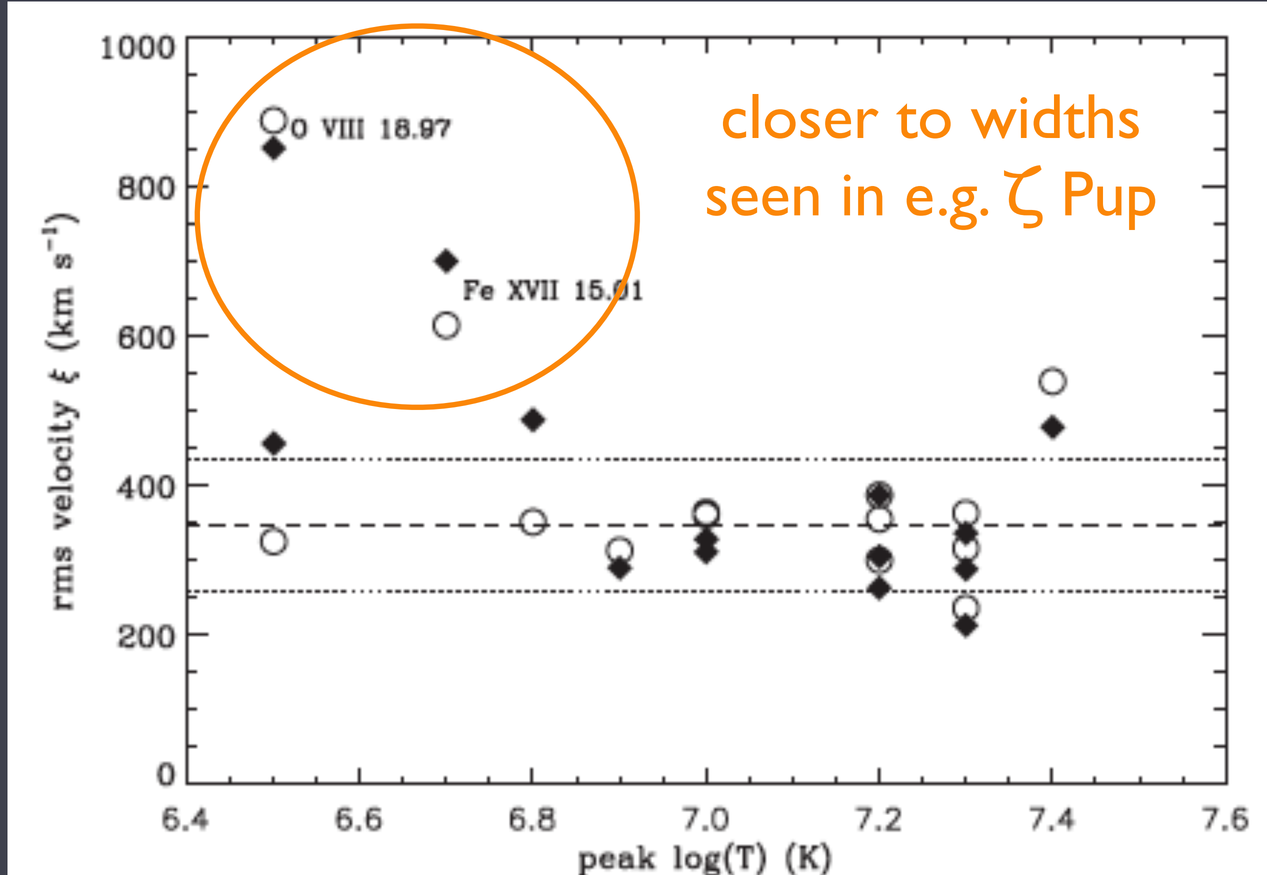


Fig. 9.—Line widths for the strongest lines in the *Chandra* spectra plotted against the temperature of peak line emissivity, taken from APED. The open circles represent the Doppler width as measured by SHERPA. The filled diamonds represent the rms velocity as measured by ISIS. The mean rms velocity and standard deviations of these lines are indicated by the horizontal lines. Note that two of the lines formed in the coolest plasma are significantly broader than the mean, but most of the lines have nonthermal line widths of a 250–450 km $s^{-1}$.

but those lines are weak in the Chandra spectrum, due to ISM attenuation

Gagné et al., 2005, ApJ, 628, 1005

# III. X-ray emission line widths and plasma kinematics

HD 148937 (Of?p) *Chandra* + *XMM* grating spectroscopy

note: *full*-width

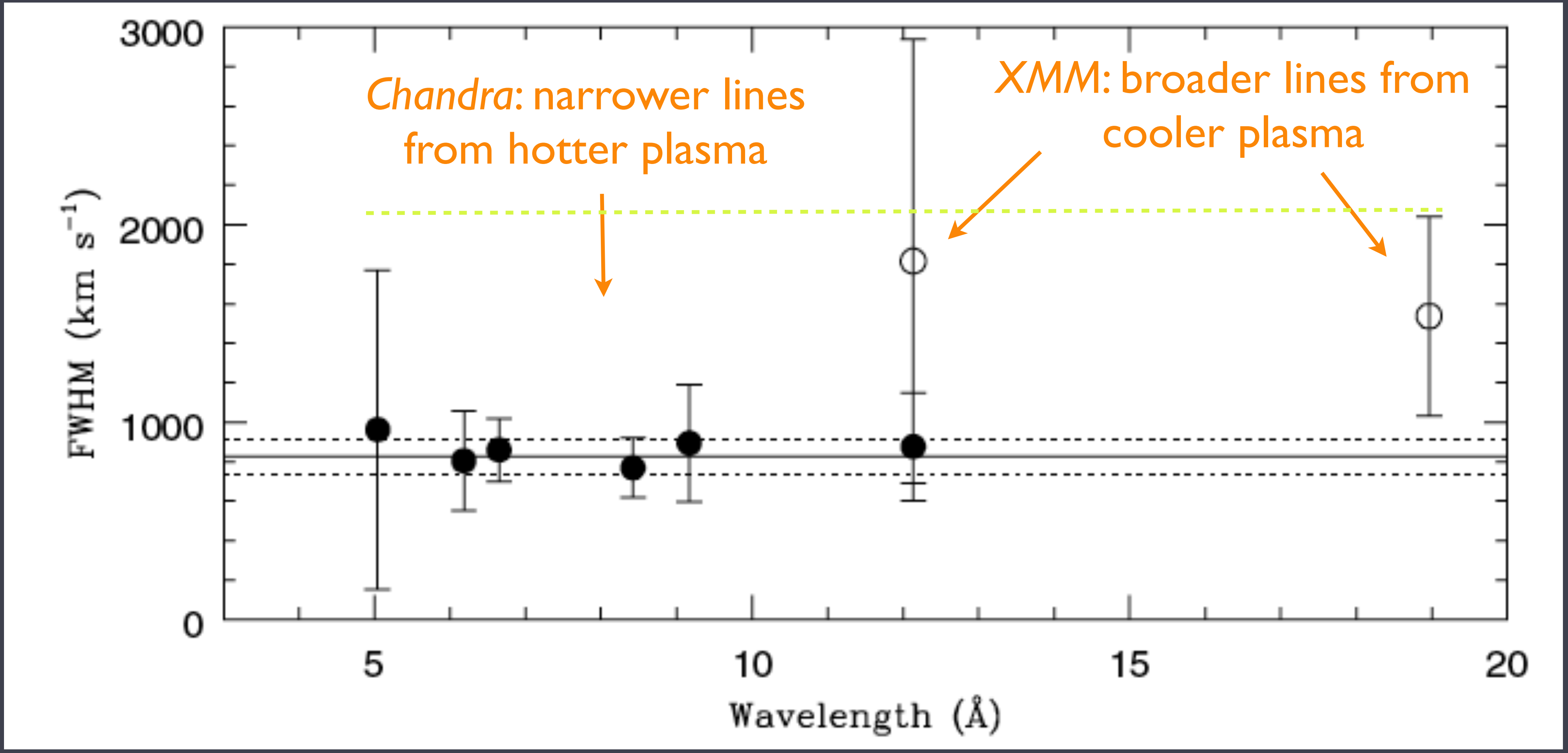


Nazé, Zhekov, & Walborn, 2012, ApJ, 746, 142

# III. X-ray emission line widths and plasma kinematics

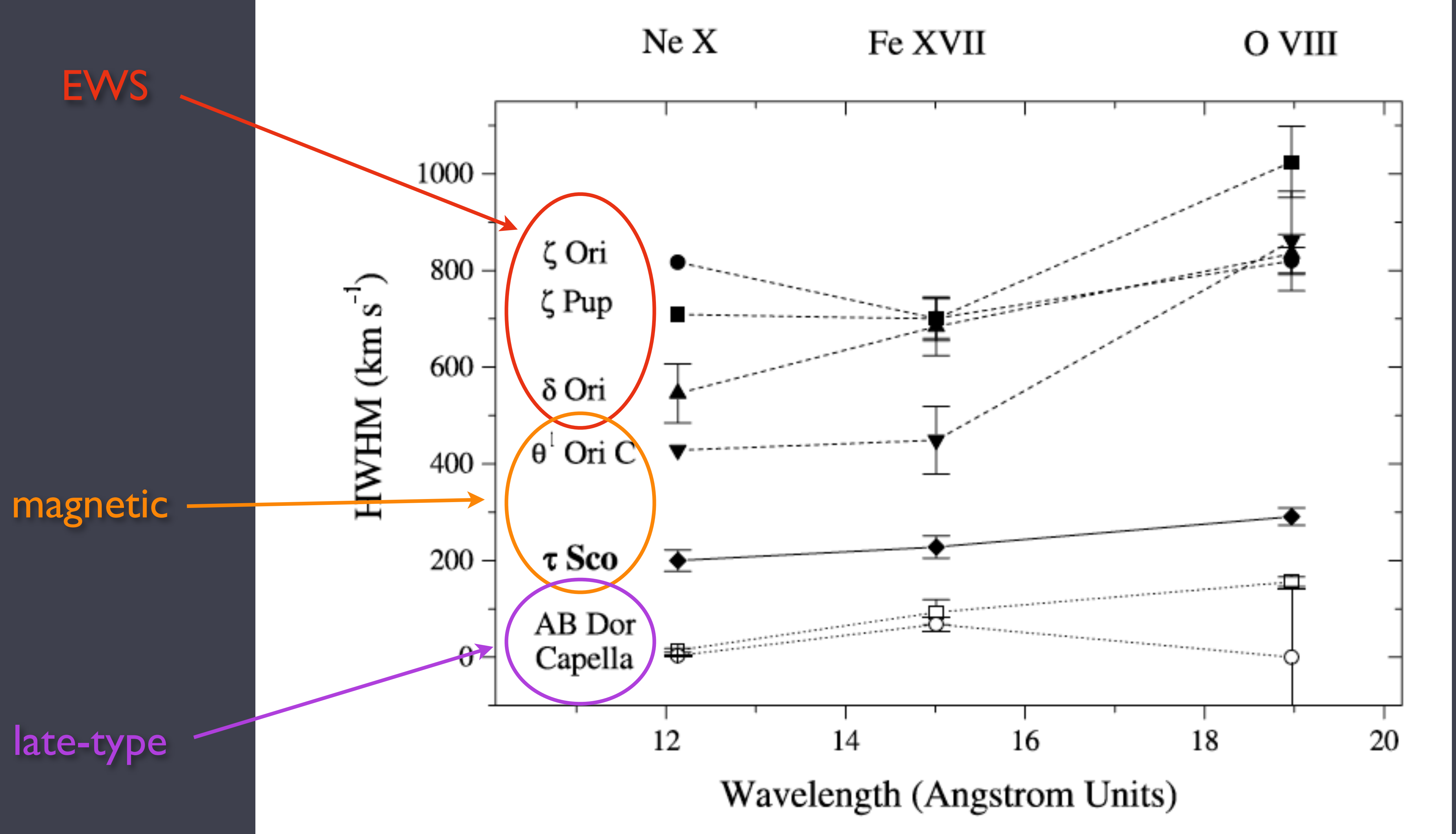


FIG. 6.—Derived line widths (HWHM) for three strong lines in seven stars: two stars representative of coronal sources (Capella and AB Dor: *open symbols connected by dotted lines*), $\tau$ Sco (*filled diamonds and solid line*), and four O stars (*filled symbols and dashed lines*), which are presumably wind X-ray sources.

Cohen et al., 2003, ApJ, 586, 495

# III. X-ray emission line widths and plasma kinematics

B (and even late O main sequence) stars may generally show narrow lines, independent of magnetism, so beware.

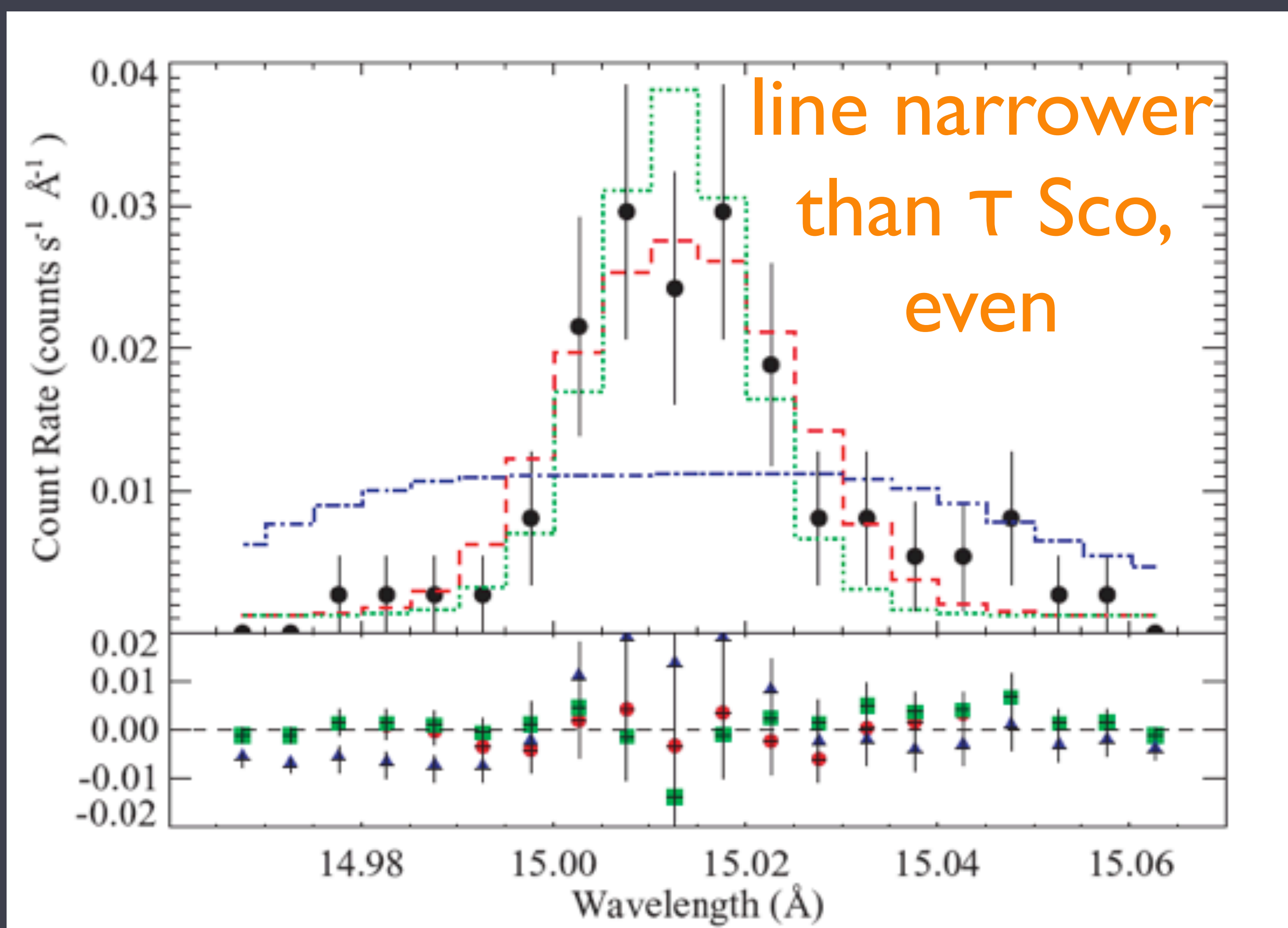


Cohen et al., 2008, MNRAS, 386, 1885

## β Cru (B0.5 III)

no field down to very low limit

**Figure 7.** The Fe XVII line at 15.014 Å with three different wind profile models. The red, dashed line is a constant velocity wind model with $v_\infty = 280\,\mathrm{km\,s^{-1}}$ (the best-fitting value for a constant outflow velocity, which produces emission lines with $v_{\mathrm{hwhm}} \approx 150\,\mathrm{km\,s^{-1}}$). The model with $v_\infty = 2000\,\mathrm{km\,s^{-1}}$, $\beta = 1$ and $R_{\mathrm{min}} = 1.5R_*$ is represented by the blue, dot–dash line. An infinitely narrow model is shown as the green, dotted line. The residuals for each model fit are shown in the lower panel, as red circles for the global best-fitting, modestly broadened ($v_\infty = 280\,\mathrm{km\,s^{-1}}$) model, green squares for the narrow profile model and blue triangles for the broad wind model. The wind model with the higher velocity ($v_\infty = 2000\,\mathrm{km\,s^{-1}}$) clearly does not provide a good fit, while the narrower constant velocity ($v_\infty = 280\,\mathrm{km\,s^{-1}}$) wind model does. Furthermore, while the very narrow model cannot be absolutely ruled out, the $v_\infty = 280\,\mathrm{km\,s^{-1}}$ model is preferred over it with a high degree of significance. All the models shown here have been convolved with the instrumental response function (RMF) and multiplied by the wavelength-dependent effective area (GARF).

# III. X-ray emission line widths and plasma kinematics

Grating spectroscopy is expensive, and current data quality is sparse and poor; this will not be a mode of discovery. But detailed study of a few stars may prove fruitful. The current challenge is for models and simulations to reproduce even the meager observations.

HWHM ~ few 100 km/s for lines coming from $T > 10^7$ K plasma; some contamination by EWS broad-line emission must be accounted for.

The focus should probably be on O stars, given the overall narrowness of X-ray lines in most/all B stars.

# IV. X-ray Variability

Rotational modulation may be expected, stochastic variability could also be present

# IV. X-ray Variability

## θ¹ Ori C: rotationally modulated X-ray emission

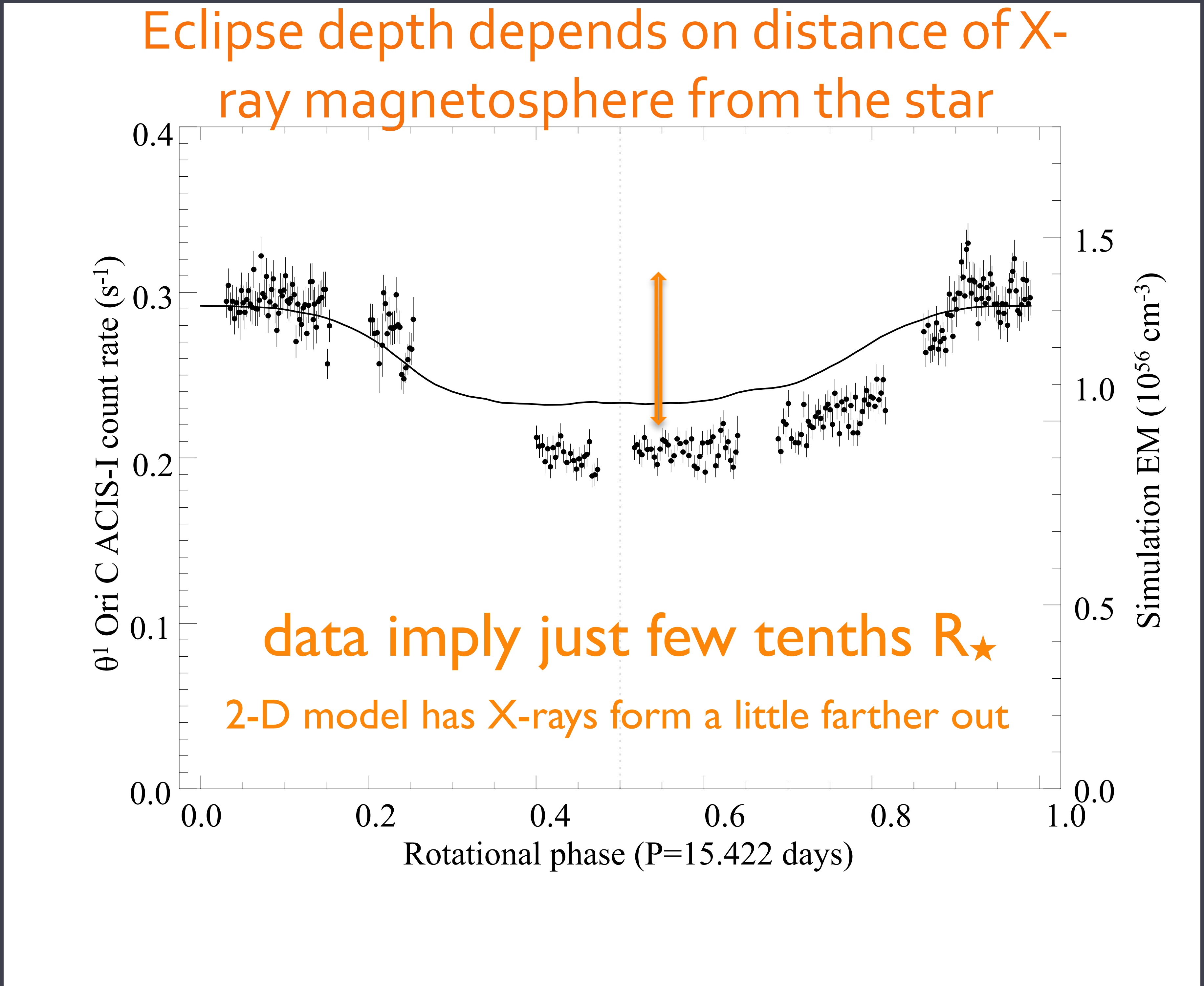

# IV. X-ray Variability

## τ Sco: variability at the 99.99% level

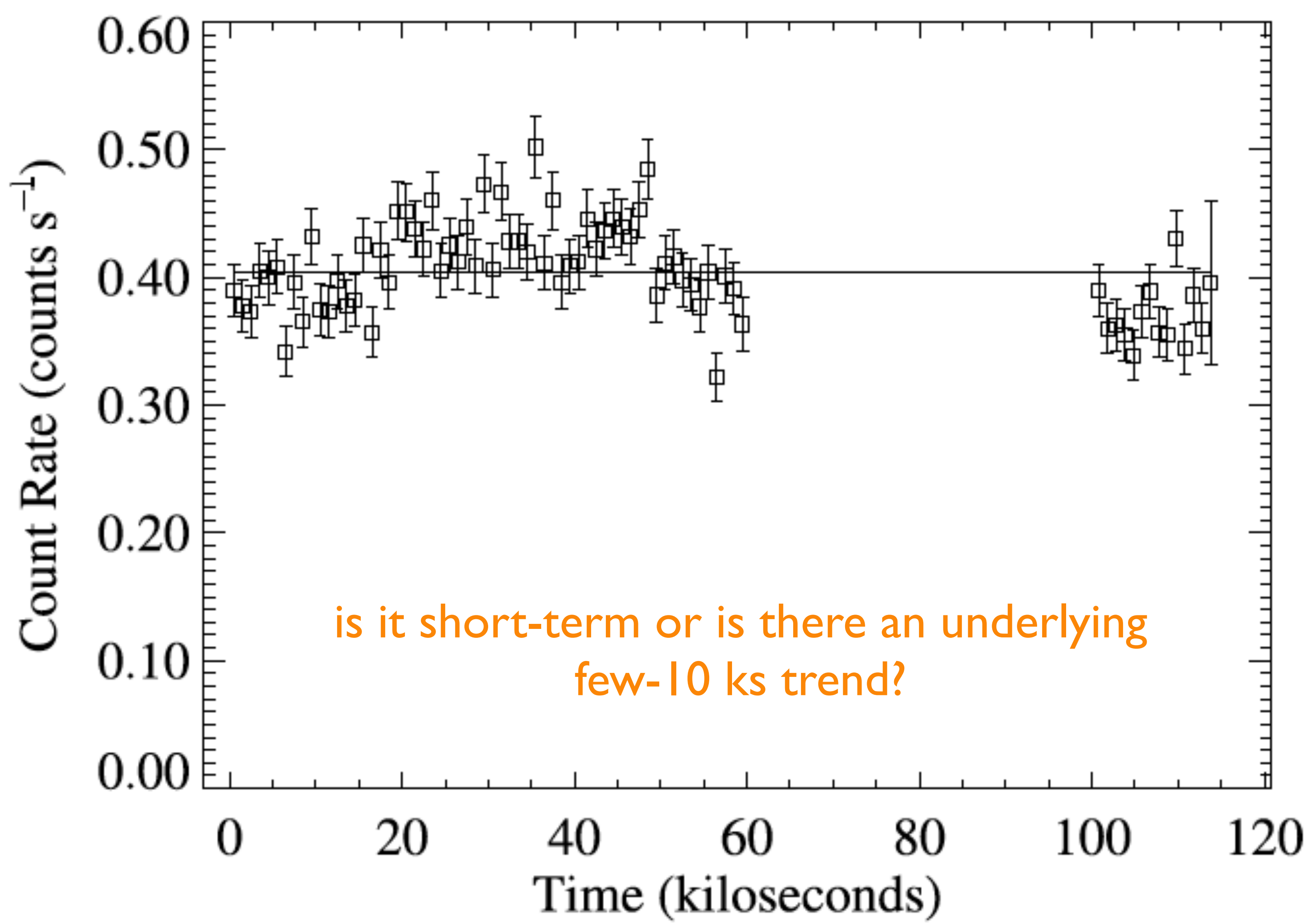


FIG. 3.—X-ray light curve formed from the combined MEG +1 and −1 order counts, with 1000 s bins. The mean count rate is indicated by the line. The hypothesis of a constant source can be rejected at a more than 99.99% confidence level.

# IV. X-ray Variability

If there are fewer sites of emission in the MCWS scenario, compared to EWS, then we might expect more X-ray variability from the former.  Perhaps on post-shock cooling timescales.

# Summary and Future Prospects

Low-resolution (CCD) spectroscopy is the only X-ray discovery mode of new magnetic stars for the foreseeable future. High Lx/Lbol, especially for O stars, may be a good indicator. Hardness may be too, but high S/N might be required to identify small amount of harder emission from magnetic processes. X-ray variability may also be a partial indicator of magnetic fields, but the level of variability seems rather low.

Detailed study at high resolution will be possible using archival X-ray grating data and also potentially newly aquired spectra from *ASTRO-H*. But only of the handful of X-ray bright magnetic OB stars in the sky (and *Chandra* and *XMM* archives).

On the next slide is the correlated ROSAT catalog of pointed observations and OB stars in the Bright Star Catalog, ranked by ROSAT count rate. This is a good reflection of X-ray flux and thus which sources have the potential to provide useful X-ray datasets. There are not many magnetic stars on the list.

**J/A+AS/118/481/table2** ROSAT all-sky survey catalogue of OB stars (Berghoefer+ 1996) ReadMe+ftp

*Post annotation*

Detections *(237 rows)*

| Full | RAJ2000 "h:m:s" | DEJ2000 "d:m:s" | HR | Name | SpType | Vmag mag | B-V mag | E(B-V) mag | log(NH) [cm-2] | Dist pc | log(Lbol) [10-7W] | OX-sep arcsec | rate ct/s |
|---|---|---|---|---|---|---|---|---|---|---|---|---|---|
| 16 | 03 08 10.1 | +40 57 20 | 936 | bet Per | B8V | 2.12 | -0.05 | 0.06 | 18.40 | 29 | 35.95 | 1.1 | 9.135 |
| 25 | 03 55 23.1 | +31 02 45 | 1209 | X Per | O9.5ep | 6.10 | 0.29 | 0.60 | 21.54 | 465 | 38.52 | 5.4 | 2.652 |
| 5 | 00 56 42.5 | +60 43 00 | 264 | gam Cas | B0IVe | 2.47 | -0.15 | 0.14 | 20.30 | 194 | 38.45 | 47.3 | 2.599 |
| 61 | 05 35 16.5 | -05 23 23 | 1895 | the1 Ori | O6p | 5.13 | 0.02 | 0.35 | 20.66 | 450 | 38.75 | 7.5 | 1.998 |
| 63 | 05 35 26.0 | -05 54 36 | 1899 | iot Ori | O9III | 2.77 | -0.24 | 0.07 | 20.30 | 501 | 39.18 | 3.1 | 1.727 |
| 53 | 05 32 00.4 | -00 17 57 | 1852 | del Ori | O9.5II | 2.23 | -0.22 | 0.08 | 20.18 | 501 | 39.34 | 6.5 | 1.667 |
| 178 | 16 35 53.0 | -28 12 58 | 6165 | tau Sco | B0V | 2.82 | -0.25 | 0.05 | 20.43 | 236 | 38.42 | 11.7 | 1.528 |
| 67 | 05 40 45.5 | -01 56 34 | 1948 | zet Ori | O9.7Ib | 2.05 | -0.21 | 0.05 | 20.48 | 501 | 39.34 | 7.9 | 1.189 |
| 141 | 13 25 11.6 | -11 09 41 | 5056 | alp Vir | B1III-IV+B2V | 0.98 | -0.23 | 0.03 | 19.00 | 86 | 37.99 | 6.0 | 1.142 |
| 104 | 08 03 35.0 | -40 00 11 | 3165 | zet Pup | O5If | 2.25 | -0.26 | 0.07 | 20.00 | 437 | 39.57 | 67.7 | 1.096 |
| 144 | 14 03 49.4 | -60 22 23 | 5267 | bet Cen | B1III | 0.61 | -0.23 | 0.03 | 19.54 | 85 | 38.10 | 9.0 | 1.085 |
| 64 | 05 36 12.8 | -01 12 07 | 1903 | eps Ori | B0Ia | 1.70 | -0.19 | 0.04 | 20.48 | 463 | 39.17 | 12.1 | 0.885 |
| 40 | 05 12 17.9 | -11 52 09 | 1696 | iot Lep | B8V | 4.45 | -0.10 | 0.01 | 19.76 | 84 | 35.87 | 14.4 | 0.864 |
| 17 | 03 27 10.2 | +09 43 58 | 1038 | xi Tau | B9Vn | 3.74 | -0.09 | 0.00 | 18.50 | 51 | 35.58 | 3.7 | 0.823 |
| 182 | 16 41 20.4 | -48 45 47 | 6187 | HD 150136 | O5III(f) | 5.65 | 0.13 | 0.45 | 21.42 | 1225 | 39.55 | 1.2 | 0.618 |
| 236 | 23 42 43.3 | -14 32 42 | 8988 | ome2 Aqr | B9.5V | 4.49 | -0.04 | 0.01 | 19.76 | 65 | 35.47 | 10.8 | 0.563 |
| 98 | 07 29 05.7 | -38 48 43 | 2875 | HD 59635 | B5Vp | 5.43 | -0.16 | 0.01 | 19.76 | 209 | 36.54 | 11.1 | 0.519 |
| 89 | 06 58 37.5 | -28 58 20 | 2618 | eps CMa | B2II | 1.50 | -0.21 | 0.02 | 18.02 | 187 | 38.16 | 7.8 | 0.514 |
| 211 | 19 36 42.4 | -24 53 01 | 7440 | 52 Sgr | B9 | 4.60 | -0.07 | 0.01 | 19.76 | 75 | 35.59 | 7.3 | 0.486 |
| 35 | 04 38 15.8 | +20 41 05 | 1471 | HU Tau | B8V | 5.92 | -0.05 | 0.06 | 20.54 | 153 | 35.87 | 1.9 | 0.460 |
| 80 | 06 22 42.0 | -17 57 21 | 2294 | bet CMa | B1II-III | 1.98 | -0.23 | 0.03 | 19.48 | 203 | 38.25 | 12.5 | 0.417 |
| 66 | 05 38 44.8 | -02 36 00 | 1931 | sig Ori | O9.5V | 3.81 | -0.24 | 0.07 | 20.56 | 501 | 38.80 | 12.8 | 0.392 |
| 127 | 10 42 57.4 | -64 23 40 | 4199 | the Car | B0Vp | 2.76 | -0.22 | 0.08 | 20.28 | 207 | 38.37 | 2.9 | 0.378 |
| 189 | 17 33 36.5 | -37 06 14 | 6527 | lam Sco | B2IV+B | 1.63 | -0.22 | 0.02 | 19.23 | 100 | 37.72 | 1.0 | 0.360 |
| 4 | 00 32 23.8 | +06 57 20 | 132 | 51 Psc | B9.5V | 5.67 | 0.00 | 0.05 | 20.46 | 105 | 35.47 | 17.8 | 0.339 |
| 41 | 05 12 55.9 | -16 12 20 | 1702 | mu Lep | B9IIIpHgMn | 3.31 | -0.11 | 0.00 | 18.50 | 61 | 35.94 | 6.5 | 0.336 |
| 180 | 16 37 09.5 | -10 34 02 | 6175 | zet Oph | O9.5Vn | 2.56 | 0.02 | 0.33 | 20.78 | 154 | 38.62 | 5.5 | 0.321 |
| 84 | 06 40 58.7 | +09 53 45 | 2456 | 15 Mon | O7V((f)) | 4.66 | -0.25 | 0.07 | 20.35 | 692 | 38.89 | 5.3 | 0.313 |
| 134 | 12 47 43.3 | -59 41 20 | 4853 | bet Cru | B0.5III | 1.25 | -0.23 | 0.05 | 20.46 | 147 | 38.43 | 71.3 | 0.311 |
| 69 | 05 47 45.4 | -09 40 11 | 2004 | kap Ori | B0.5Ia | 2.06 | -0.17 | 0.04 | 20.58 | 567 | 39.06 | 4.6 | 0.302 |
| 58 | 05 35 08.3 | +09 56 03 | 1879 | lam Ori | O8III((f)) | 3.54 | -0.18 | 0.13 | 20.87 | 501 | 39.01 | 9.0 | 0.300 |
| 190 | 17 34 42.5 | -32 34 54 | 6535 | V1036 Sco | O7V+O7V | 5.70 | 0.04 | 0.36 | 21.32 | 800 | 38.98 | 1.0 | 0.291 |
| 54 | 05 31 55.9 | -07 18 06 | 1855 | ups Ori | B0V | 4.62 | -0.26 | 0.04 | 20.35 | 494 | 38.33 | 3.4 | 0.267 |
| 34 | 04 33 33.0 | +18 01 00 | 1442 | | B9IVn | 6.25 | 0.07 | 0.14 | 20.91 | 157 | 35.79 | 9.9 | 0.254 |
| 27 | 03 58 57.9 | +35 47 28 | 1228 | xi Per | O7.5III(n)(( | 4.04 | 0.01 | 0.32 | 21.06 | 398 | 38.90 | 8.0 | 0.220 |
| 136 | 13 06 16.7 | -48 27 48 | 4940 | | B5V | 4.71 | 0.14 | 0.03 | 20.24 | 145 | 36.54 | 21.0 | 0.219 |

prospects for high S/N X-ray spectroscopy

ROSAT/ Bright Star Cat. sorted by X-ray count rate